energies

Article

Thermal Transmittance in Roof–Wall Structural Junction Areas Insulated with a Hemp–Lime Mixture

Magdalena Grudzińska, Krystian Patyna, Wojciech Jabłoński and Przemysław Brzyski *

Faculty of Civil Engineering and Architecture, Lublin University of Technology, 40 Nadbystrzycka St., 20-618 Lublin, Poland; m.grudzinska@pollub.pl (M.G.); k.patyna@pollub.pl (K.P.); w.jablonski@pollub.pl (W.J.)
* Correspondence: p.brzyski@pollub.pl; Tel.: +48-815-384-448

Abstract: The junction between the roof and the external wall is a sensitive area within the building envelope; here, increased heat flow often takes place. In the case of partitions insulated with materials based on plant ingredients, thermal bridges are particularly dangerous due to the possibility of condensation and, consequently, mold. The present article analyzed the connection of the roof with the knee wall made of a hemp–lime composite and the ridge in terms of the occurrence of thermal bridges. The following factors that may affect heat transfer in the junction were taken into account: the location of the load-bearing wooden frame, the roof slope, and the presence of internal plaster in the junction. Two-dimensional heat transfer analysis was performed based on the finite element method using THERM 7.4 software. All of the studied thermal bridges had ψ values below 0.10 W/(m·K). Calculations of heat losses through a roof with different slopes were also presented, taking into account the considered thermal bridges. As the roof slope decreases, the heat flow through the roof decreases, despite the increasing value of the linear thermal transmittance. The share of the considered thermal bridges in the total heat loss from the roof reached up to 15%. To verify the obtained results, in further analysis, it would be necessary to calculate the impact of the roof–knee wall bridge variants on heat losses throughout the entire building.

Keywords: hemp–lime composite; thermal bridge; heat losses; roof; ridge; structural junction

check for updates

Citation: Grudzińska, M.; Patyna, K.; Jabłoński, W.; Brzyski, P. Thermal Transmittance in Roof–Wall Structural Junction Areas Insulated with a Hemp–Lime Mixture. *Energies* **2024**, *17*, 316. https://doi.org/10.3390/en17020316

Academic Editor: Francesco Nocera

Received: 26 November 2023
Revised: 23 December 2023
Accepted: 3 January 2024
Published: 8 January 2024

1. Introduction

One of the dominant directions in the global climate policy is the reduction in energy consumption and the decrease in the carbon footprint in the construction industry. According to various estimates, this sector accounts for 30–40% of all energy consumption and between 27% and 30% of greenhouse gas emissions [1–5]. The Paris Agreement (Accord de Paris), resulting from the United Nations Framework Convention on Climate Change (UNFCCC), stands as a pivotal agreement concerning the limitation of global warming. It obliges member states to reduce greenhouse gas emissions, significantly impacting the construction sector by promoting the energy efficiency of buildings [6].

The European Green Deal, as one of the most crucial European policies, represents the European Union's strategic plan aiming to achieve climate neutrality by 2050. Within this framework lies the Renovation Wave, imposing a series of actions and standards to enhance the energy efficiency of existing buildings. The Directive on the Energy Performance of Buildings (2002/91/EC) [7], amended in 2023 (2023/1791/EU) [8], stands as a key legal act at the European level, specifying minimum requirements regarding the energy performance of buildings. Through these agreements and directives, the European Union and the international community take steps to reduce emissions and enhance the energy efficiency of the construction sector, contributing to global efforts for sustainable development. According to Trotta's estimations, energy consumption by buildings in the EU should decrease by 30% by 2030 [9].

One of the ways to improve the energy efficiency of buildings, besides increasing the thermal insulation of building partitions, is the elimination of or reduction in thermal bridges. Theodosiou et al. observed that the omission of thermal bridges in thermal insulation calculations leads to a 30% increase in energy consumption [1,10]. However, these estimates vary depending on the region in which the studies were conducted. For instance, Kotti et al. [11] observed a 13% energy loss due to thermal bridges in residential buildings in Greece. Evola et al., in their research estimating energy loss costs in the Mediterranean climate due to thermal bridges, indicated a potential 17.5–25% savings in heating energy upon reducing thermal bridges [12].

Furthermore, as indicated by Ilomets et al. [13], based on studies of existing residential buildings, the occurrence risk of surface vapor condensation due to thermal bridges is approximately 49–51%, depending on the construction technology used. Condensation of water vapor in building partitions can lead to mold and other fungal developments within the building [1,10,13–16]. This phenomenon adversely affects the health and comfort of occupants, leading to serious respiratory, rheumatic, and allergic conditions [17,18].

The issue of thermal bridges is widely recognized; however, many studies focus on those occurring in walls and their connections with other building elements. Issues related to thermal bridges in roofs are much less frequently addressed.

The most prevalent problem associated with thermal bridges in roofs involves the occurrence of linear thermal bridges on rafters and at the junction between the actual thermal insulation and the structural elements of the roof truss. It is important to note that, in the traditional model of thermal insulation, where the insulation layer is placed between rafters, structural heterogeneity occurs. In these areas, thermal bridges form within the insulation layers near wooden elements [19]. Despite wood having a relatively low heat transfer coefficient ranging from 0.16 to 0.30 W/(m·K) [19], it possesses thermal properties that are significantly worse than those of standard insulation materials, such as mineral wool, which has a heat transfer coefficient ranging from 0.030 to 0.040 W/(m·K).

The contemporary requirements for thermal insulation, stemming from national and international regulations, incline towards solutions involving additional layers of thermal insulation. For technological reasons and installation convenience, an additional insulation layer is often placed within the partition, between the frames intended for the installation of plasterboard panels. This placement results in structural wooden elements being located in cold-temperature layers. The lack of insulation continuity at the knee wall encourages the formation of thermal bridges at the junctions between the building's structural elements. Also, the occurrence of condensation at negative temperatures in these areas is likely to damage the structure due to the expansion of water within the material's capillary pores [19].

The transitioning of surfaces, such as in chimneys or any installation openings, leads to a breach in the integrity of thermal insulation, resulting in the formation of thermal bridges. The solution lies in minimizing the number of penetrations through the insulation layers.

Any discontinuity of surfaces in building construction generates geometric thermal bridges by increasing the external surface area of the partition compared to the internal part. These areas primarily occur at the junctions of external walls with the roof and in the ridge [1,15,20]. The junction of the truss with the wall also poses a problem due to the use of different insulation materials of varying thicknesses. Modern architectural concepts, devoid of roof gutters (known as hidden gutters), often exacerbate this issue.

With the growing interest and a policy-driven approach towards improving the energy efficiency of buildings, technologies are being developed to enhance material insulation while simultaneously reducing the carbon footprint of production. One such method involves the utilization of hemp fibers or shives in building materials such as hemp wool insulation, blown insulation in the form of blocks, or in the form of the discussed hemp–lime composite cast in formwork on the construction site.

In light of the subject of the present article, the main thermal and moisture parameters of the hemp–lime composite are presented below. The primary component of the mixture, hemp shives, is characterized by a high porosity level, reaching 78% [21]. Empirical and computational scientific studies thus far unambiguously indicate that the porosity of materials significantly affects the thermal conductivity [22–25]. The high porosity contributes to the hemp shives having a low thermal conductivity, with a coefficient of lambda at the level of 0.05 W/(m·K) [21]. The composite, consisting of a mixture of hemp shives, hydrated lime, metakaolin, and gypsum, can exhibit a thermal conductivity coefficient ranging from 0.07 W/(m·K) to 0.138 W/(m·K), depending on the applied proportions [26–28]. The increase in the lambda coefficient is a result of the higher density of the mixture. Mixtures characterized by increased compressive strength tend to have reduced insulation properties [29,30]. An additional aspect arising from the porosity of the composite is its low diffusion resistance, leading to a natural ability to regulate air humidity in indoor spaces [31]. Similarly to thermal parameters, the diffusion resistance decreases with an increase in the density of the mixture.

The embodied energy of the hemp–lime composite, considering the entire production process, is relatively lower compared to traditional thermal insulation materials such as polystyrene, mineral wool, or wood wool. The amount of embodied energy directly translates into the quantity of CO_2 emitted during the material's life cycle.

The lower energy requirement for the production of hempcrete stems from several factors. One of the initial and significant factors is the production process of the primary raw material, industrial hemp. Apart from the energy required for transportation, sowing, and field processing, the absence of the need for fertilization is crucial, resulting in a low energy requirement for the production of fertilizers. During the growth phase, hemp plants sequester carbon dioxide. Roughly, from one hectare of cultivation, 7–10 tons of hemp shives can be obtained [32].

Assuming that one ton of material can sequester approximately 1800 kg of CO_2 [28], one hectare of cultivation would impound between 12.6 and 18 tons of CO_2. The sequestered carbon dioxide is not subsequently released.

Other components of the hemp mixture, such as hydrated lime, metakaolin, and gypsum, require significant energy inputs during the production process. Hydrated lime, constituting 75% of the binder mixture mass, is a significant factor in terms of energy consumption, primarily due to its substantial use among the components. A factor that partially offsets CO_2 emissions during production is the fact that lime rebinds CO_2 during the curing process of the hemp concrete mixture [33].

The components mentioned above, when combined with water, form hemp concrete. The total amount of emitted carbon dioxide, despite processes related to the production of hemp shives and lime, varies between −0.3 and −1 kg CO_2 per kilogram of the mixture, depending on the mixture's density [34]. For comparison, traditional insulation materials such as expanded polystyrene (EPS), glass wool, and polyurethane foam exhibit a high carbon emission coefficient due to their production processes and use of non-renewable resources. The CO_2 emission coefficient per kilogram varies depending on the assumptions made, with values ranging from 5.05 kg to 8.25 kg CO_2 for expanded polystyrene, from 2.77 to 3.62 kg CO_2 for glass wool, and 5.31 kg CO_2 for polyurethane foam (per kilogram of product, respectively) [35].

Wood wool, considered an environmentally friendly material, also has an increased carbon emission coefficient compared to the hemp–lime composite, standing at 1.56 kg CO_2 per kilogram of the product [35].

As indicated by the referenced literature, hempcrete, when used as thermal insulation for buildings, demonstrates favorable thermal properties. Furthermore, it exhibits good CO_2 emission coefficients compared to traditional insulation materials, which is significant in the context of reducing emissions in the construction sector. Therefore, further research is necessary to determine the essential parameters for achieving this goal.

The aim of this work is to present simulated two-dimensional models of thermal bridges in the area of roof–wall and ridge connections. The analyzed junctions differ in the location of the load-bearing wooden frame in relation to the wall thickness, the slope of the roof, and construction details inside the core of bridges. Temperature distribution in the described construction junctions was calculated using the THERM 7.4 software. It was the basis for further analyses of the linear thermal transmittance coefficients, showing excessive heat transfer above the level typical for flat building partitions without any intrusions. Additionally, heat losses through an exemplary roof were calculated. The thermal parameters of the composites used in the studies were taken from the authors' own laboratory tests. The presented analyses concerning the roof–wall junctions in a construction insulated with a hemp–lime composite are the novelty of the research and a continuation of previous work [4,15,19] on other junctions in this construction technology.

2. Materials and Methods

2.1. Junctions Used in Calculations

The presented sections of the building partitions were evaluated as a continuation of the authors' previous research concerning thermal bridges in hemp–lime constructions [4,15,19]. The earlier publications described the construction details, such as the wall–ceiling connection, the window placement in a wall, the floor on the ground, and the foundation wall. The roof construction details, such as the wall plate with a knee wall and a ridge, are equally important in analyses of the energy demands of ecological buildings, and may significantly contribute to the heat losses from the upper part of the building.

External walls were assumed to have a timber frame positioned centrally in relation to the wall thickness (variant "a"—Figure 1), and in the second case, it was positioned on the internal side of the wall (variant "b"—Figure 2). Both types of walls were insulated with a hemp–lime composite layer that was 400 mm or 530 mm thick (variant I and II). The wall was finished with lime plaster from the outside and clay plaster from the inside. These solutions are commonly used in practice. The junction of the roof slopes in the ridge was also modeled (Figure 3). The roof was insulated with a light hemp–lime mixture placed between the rafters. At the bottom, additional insulation made of wood wool was placed between wooden battens. Figures 1–3 show details with a roof inclined at an angle of 20°, while variable inclinations of 10°, 20°, 30°, and 40° were assumed in the work.

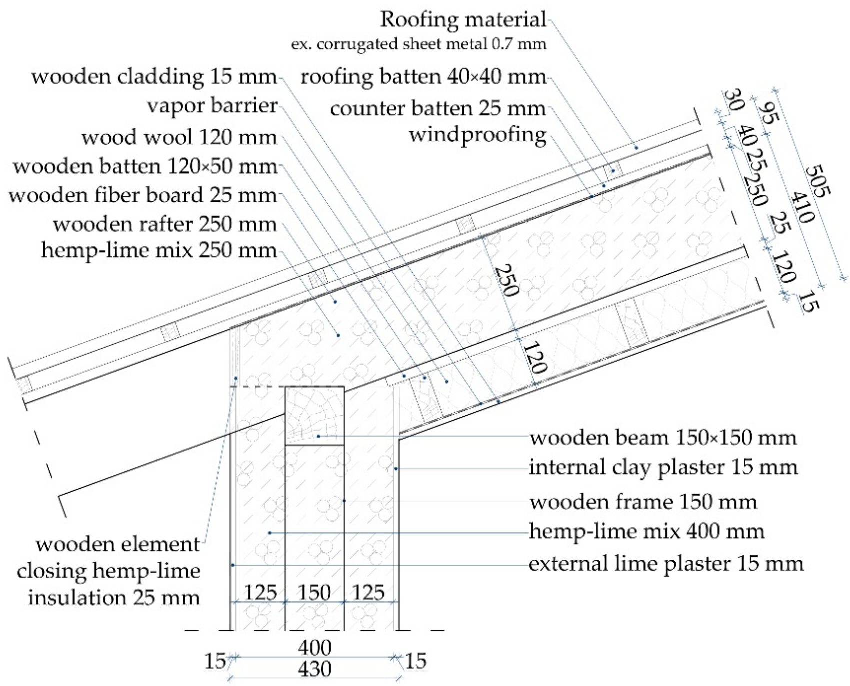

Figure 1. Connection of the wall and roof with the timber frame located centrally in relation to the wall thickness (variant "a" of wall construction).

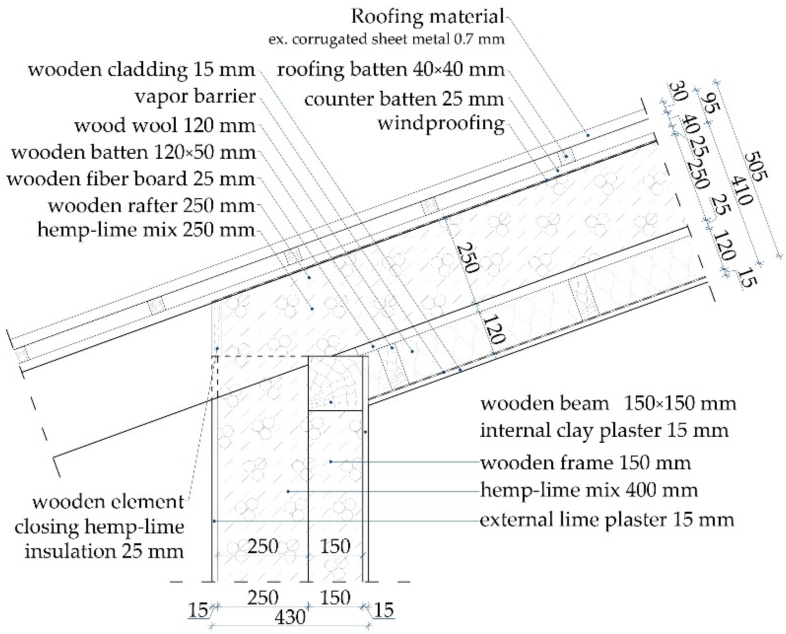

Figure 2. Connection of the wall and roof with the timber frame on the inner side of the wall thickness (variant "b" of wall construction).

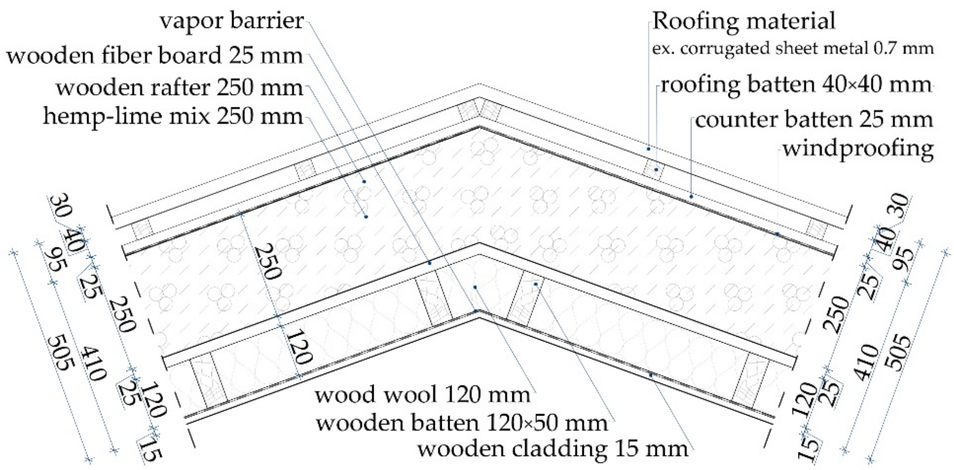

Figure 3. Detail of the roof connection in the ridge.

2.2. Simulations

2.2.1. Calculation Method

Comparative analyses of the construction junctions require a two- or three-dimensional model of heat transfer, allowing for their qualitative and quantitative evaluation. The qualitative examination may cover a visual comparison of the isotherm layout and the heat flux vectors in the connection. Quantitative assessment is based on the linear thermal transmittance values, characterizing the additional heat transfer compared to the heat transfer in uniform building partitions of the same length, as in the modelled junction.

In this paper, two-dimensional models of thermal bridges were prepared in line with the standard ISO 10211 [36] using THERM 7.4 software. The software is developed and distributed by the Lawrence Berkeley National Laboratory (LBNL) for use by building component manufacturers, engineers, architects, and others interested in heat transfer [37].

Validation of the code was presented in [38]. It was made according to the standard ISO 10211 [36] and consisted of comparing the numerical results of the temperature at specified grid junctions given by the program with a strict analytical solution. For a code to be classified as a "high precision calculation method", the temperature should not differ by more than 0.1 K compared with the values listed in the standard; additionally, heat flow should not vary by more than 0.1 W/(m·K) from the given heat flow. The program complies with all requirements of the norm [36]. In the analyses of thermal bridges, the experimental validation of the models is not commonly practiced, as this would require constructing a costly, large-scale model [39,40]. Additionally, difficulties in maintaining stable temperature conditions during the measurements and eliminating boundary effects would make it difficult to obtain reliable results.

Numerical calculations of the temperature and heat flux in the construction junctions prepared with the use of the THERM 7.4 software include the following: the introduction of 2D geometric data through a graphic interface [41], the definition of material properties and boundary conditions, the generation of a mesh within the element, the computation of heat transfer through the Finite Element Analysis Solver, and the presentation of the processed results. The basis for the further analyses is mainly the isotherm profile and the thermal transmittance coefficient (U [W/(m^2·K)]), averaged for the whole length of a thermal bridge.

The modelled connection of building partitions forms a core of the bridge, where the heat transfer is two-dimensional. One-dimensional heat transfer should be restored at some distance from this center, usually estimated as a threefold thickness of the partitions (and no less than 1 m) [36]. The cut-off planes are considered to be adiabatic, which means that there is no heat transfer through them, and the isotherms are perpendicular to the planes.

The linear thermal transmittance coefficient ψ [W/(m·K)] may be determined using the internal or external dimensions of the junction. Its value depends on the thermal flux transferred per length and temperature units of the bridge in steady-state conditions [42]. The specific values are then subordinated to the method of the calculation of energy demand, based on the internal or external dimensions of building partitions. In the case of convex junctions, external ψ values are usually negative, because their external boundaries are typically longer than the internal boundaries. This may make the analyses more difficult, as the results are sometimes not intuitive or clear enough to be appraised. The internal ψ values are commonly positive, giving a more evident idea of the range of thermal losses through the construction. In the analyses, the linear thermal transmittance coefficient was calculated according to EN ISO 10211 [36] using internal dimensions according to Equation (1):

$$\psi_i = L^{2D} - \sum_j L_j \cdot U_j \tag{1}$$

where: L^{2D}—thermal coupling coefficient obtained from the 2D analysis of the modelled element as a multiplication of the averaged thermal transmittance U and the junction's length [W/(m·K)]; j—number of building partitions connecting in the thermal bridge; L—internal length of a building partition [m]; U—thermal transmittance coefficient of a building partition [W/(m^2·K)].

Calculations of thermal transmittance of building partitions (walls and roof) were made with the use of the standard ISO 6946 [43] and the THERM 7.4 software. The work focused on the 2D simulations, and some effects connected with 3D heat flow in the rafters and roof insulation were neglected. According to [44], the error resulting from performing 2D instead of 3D simulations in the case of a knee wall–roof junction was approximately 9%. The analyses were made for the building with a Porotherm block wall construction (including reinforced concrete elements) and a rafter roof. The biggest influence on the error was found to be the thermally diversified wall construction, and for the more homogenous roof part, it did not exceed 3%. In the presented case, the wall is more uniform in terms of the thermal properties of its parts. The thermal conductivity of insulating materials with organic components (hemp–lime mixtures) is 0.08 W/(m·K), and the thermal conductivity of timber forming a thermally weaker element is equal to 0.16 W/(m·K).

To make the influence of the 2D calculation method smaller, the following procedure was introduced for all of the partitions including non-uniform layers, such as a wooden load-bearing frame filled with the hemp–lime composite in the walls, rafters filled with the hemp–lime mix, and wood wool between wooden battens fixed below the rafters in the roof construction. These layers were modelled in THERM first (cross-sections perpendicular to the timber elements), presuming there is no thermal resistance between the outer boundaries of the layers and the internal or external environment. Then, their averaged thermal transmittance coefficients were used to calculate substitutive thermal conductivity and applied in further THERM work.

2.2.2. Materials' Properties and Boundary Conditions Used in Calculations

Tables 1 and 2 present the thermal conductivity of materials and elements assumed in modelling, together with boundary conditions. The thermal conductivity of the hemp–lime mixtures was obtained from the authors' own research and laboratory measurements [4,15,19,21]. The source of the thermal conductivity coefficients of other materials was the ISO 10456 standard [45] or the catalogues of manufacturers. The absolute error of the numerical analyses (calculated as the absolute value of the difference between the heat inflow and outflow, divided by the mean heat flux through the junction) did not exceed 0.01%.

Table 1. Thermal conductivities of materials and building products.

Building Material	Thermal Conductivity λ [W/(m·K)]
Hemp–lime mix (wall)	0.080
Hemp–lime mix (roof)	0.065
Wood wool	0.038
Timber	0.16
Fiberboard (low density)	0.07
Lime or clay plaster	0.70

Table 2. Boundary conditions assumed in modelling.

Surface	Temperature [°C]	Surface Resistance [(m^2·K)/W]	Description
Internal surface of the wall	+20	0.13	Heat flow horizontal, simplified *
Internal surface of the roof	+20	0.10	Heat flow upwards, simplified *
External surface (walls and roof)	0	0.11	Simplified *
Cut-off planes	–	–	Adiabatic

Note: * the simplified model means that convective and radiative heat exchange is described by one common surface resistance.

According to the Polish Institute of Meteorology and Water Management, the mean external winter temperature in Poland during 1991–2020 was −0.4 °C, and during 2020–2021, it was −0.2 °C [46]. Regarding the rising trend of the air temperature in Poland, the external temperature in the simulations was set to 0 °C to obtain the internal temperature in the junctions consistent with average winter conditions. The external temperature does not have any influence on the linear thermal transmittance coefficient, as it is adjusted to the unitary temperature difference.

The external surface resistance R_{se} was calculated according to the ISO 6946 standard [43], as in Equation (2).

$$R_{se} = \frac{1}{h_c + h_r} \quad (2)$$

where h_c—the convective coefficient, for external surfaces adjacent to a well-ventilated air layer [W/(m^2·K)]; h_r—the radiative coefficient, for the emissivity of surfaces of 0.9 and a given mean temperature [W/(m^2·K)].

3. Results and Discussion

Two levels of thermal insulation of the partitions that were included in the study (Table 3) cover the range of the applicability of the hemp–lime constructions in Poland. The first variant fulfills the national requirements regarding energy saving, and the second one is equivalent to the recommendations for low-energy buildings and the boundary technological requirements concerning hemp–lime walls. It is recommended that the wall thickness does not exceed approximately 500 mm [32] to enable proper drying and binding of the composite (in the second case, the thickness of the walls, excluding the plaster, is 530 mm).

Table 3. Thermal transmittance coefficients of the partitions.

Type of Partition	National Regulations [W/(m^2·K)]	Adopted Values (Variant I) [W/(m^2·K)]	Low-Energy Buildings [W/(m^2·K)]	Adopted Values (Variant II) [W/(m^2·K)]
External wall type "a"	0.20	0.198	0.15	0.147
External wall type "b"	0.20	0.198	0.15	0.148
Roof	0.15	0.149	0.12	0.117

3.1. Linear Thermal Transmittance of the Analysed Bridges

To make the results of the thermal bridges modelling more comparable, the connections of the partitions were designed to have the same internal length while calculating their linear thermal transmittance. Because of that assumption, in some of the junctions, it was necessary to add additional wooden wedges supporting the rafters placed above the capping beam. Also, the first batten supporting the ceiling was added at the same distance from the wall in all cases.

The presented junctions of the building elements with the hemp–lime mix are rather well-insulated. The thermally "weaker" parts are the wooden components, forming the load-bearing construction or upholding the roof insulation below the rafters and the internal cladding. The wooden elements such as the capping beam or the wooden battens (perpendicular to the plane of the model) deform the isotherms slightly, but their influence is not big (Figure 4).

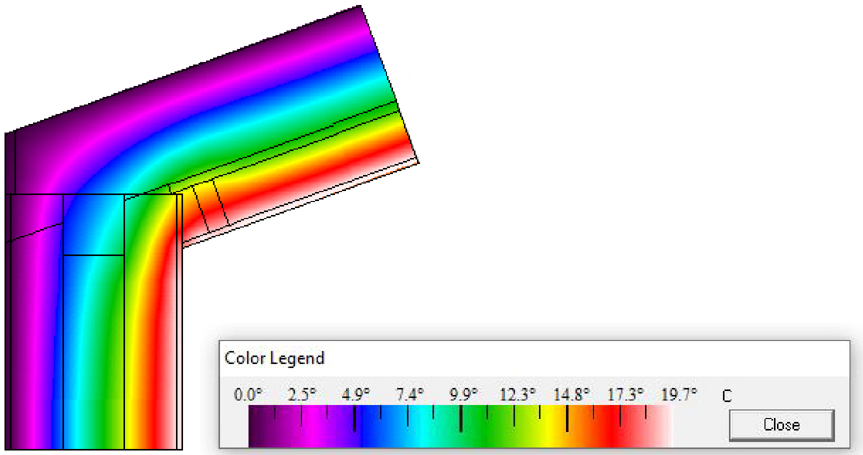

Figure 4. Schematic view of isotherms in a knee wall–roof junction (partitions cut closely to the center of the junction to make the figure smaller).

The first variants of the junction have the internal plaster put on the whole height of the wall. In this way, there is no need to measure the predicted level of the internal cladding or complement the plaster after the finishing of the roof. However, it turned out that the plaster forms a kind of slab, transferring heat into the connection much better than the surrounding elements. This phenomenon may be seen as the increased heat flux area in Figure 5.

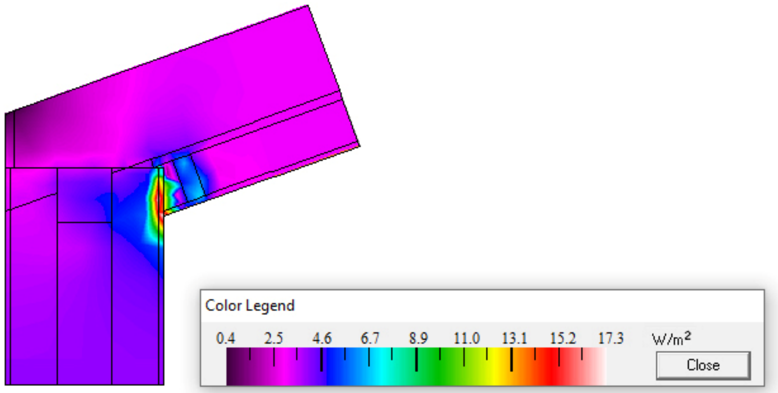

Figure 5. Schematic view of heat flux in a knee wall–roof junction (partitions cut closely to the center of the junction to make the figure smaller).

This is the reason that explains why the analyses were broadened by the alternative approach to finishing the construction, with the internal plaster applied only to the level of the connection with the ceiling (Figure 6). The values of the linear thermal transmittance are put together in Tables 4 and 5.

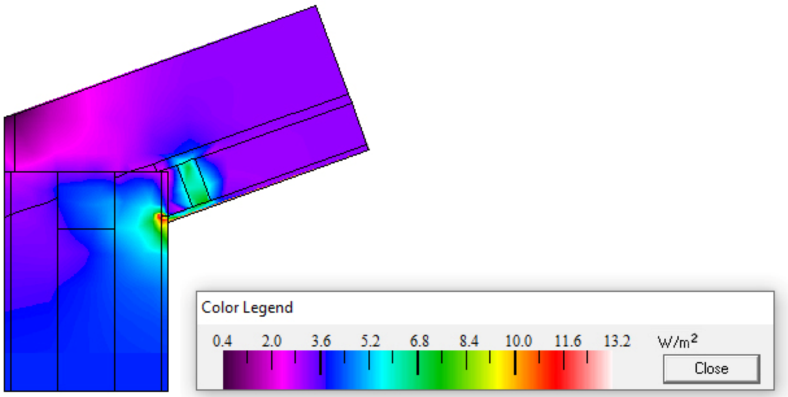

Figure 6. Schematic view of heat flux in a knee wall–roof junction after removing part of the internal plaster (partitions cut closely to the center of the junction to make the figure smaller).

The bigger the slope of the roof, the smaller the ψ value. This may be caused by the change of the geometry, getting nearer to the flat partition, and by the smaller area of the heat outflow. The values obtained for the roof sloped by 10° are close to the ISO 14683 standard [47] values for the convex corners, equal to 0.05 W/(m·K). Increased thermal insulation results in smaller ψ values as well, and the reduction ranges from 5% to 15%.

Table 4. Linear thermal transmittance (internal dimensions)—knee walls and the roof, variant I of insulating properties.

Slope of the Roof [deg]	Linear Thermal Transmittance [W/(m·K)]			
	Wall with the Central Load-Bearing Frame (Variant "a")		Wall with the Internal Load-Bearing Frame (Variant "b")	
	Plaster to the Top of the Wall	Plaster to the Ceiling Level	Plaster to the Top of the Wall	Plaster to the Ceiling Level
10	0.055	0.044	0.059	0.047
20	0.047	0.041	0.052	0.047
30	0.040	0.037	0.046	0.043
40	0.031	0.031	0.037	0.037

Table 5. Linear thermal transmittance (internal dimensions)—knee walls and the roof, variant II of insulating properties.

Slope of the Roof [deg]	Linear Thermal Transmittance [W/(m·K)]			
	Wall with the Central Load-Bearing Frame (Variant "a")		Wall with the Internal Load-Bearing Frame (Variant "b")	
	Plaster to the Top of the Wall	Plaster to the Ceiling Level	Plaster to the Top of the Wall	Plaster to the Ceiling Level
10	0.048	0.037	0.053	0.042
20	0.042	0.036	0.047	0.041
30	0.036	0.033	0.042	0.040
40	0.029	0.029	0.035	0.035

Removing the plaster from the inside area of the bridge reduced the linear thermal transmittance by 20–23% at the maximum (slope of the roof 10°) for both types "a" and "b" of wall construction (Figure 7). In the case of the roof sloped by 40° the ψ values remained the same. Here, the wall corner dipped very little during the roof construction; therefore, in practice, it would be not justifiable to lay the plaster to a lower level.

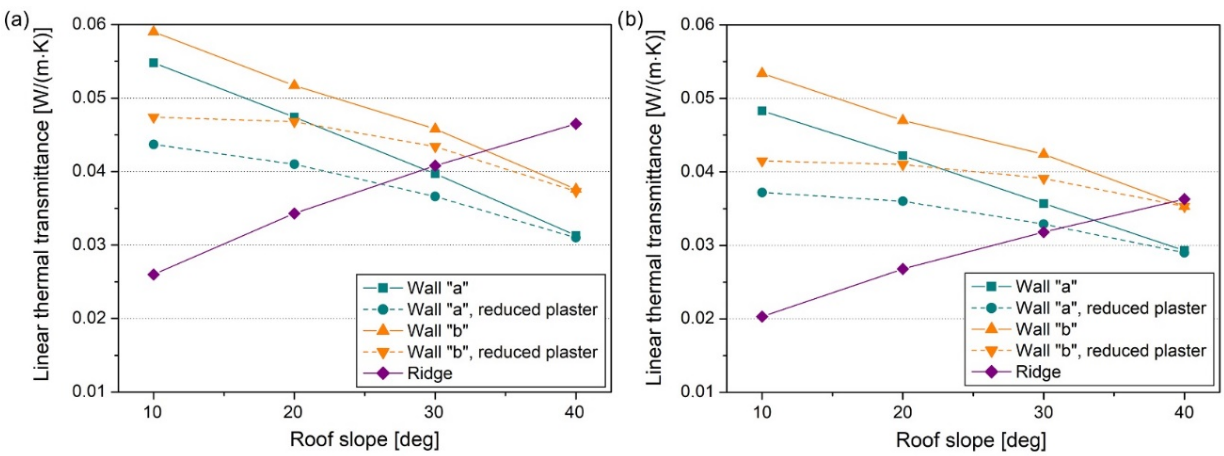

Figure 7. Linear thermal transmittance of the analyzed junctions: (**a**) variant I of insulating properties; (**b**) variant II of insulating properties.

The connection of the wall with the load-bearing frame located near its inner surface and the roof turned out to be a worse solution concerning the thermal bridge in the corner. The steeper the roof, the bigger the difference that occurred between variants "a" and "b", ranging from approximately 8% (slope 10°) to 22% (slope 40°). This was probably caused by the presence of the additional wooden wedges supporting the rafters placed on the capping beam. Their application was necessary to keep a constant level of the roof above the knee wall and a constant length of the partitions creating the junction. In addition, the type "b" wall construction has a slightly higher thermal transmittance coefficient than the type "a" construction, which may also contribute to this effect.

Concerning the ridge, a similar regularity may be observed as for the knee wall—the more convex the shape of the junction, the bigger the linear thermal transmittance (Table 6). The smallest slope (10°), close to the plane, is characterized by the smallest ψ value. This may suggest that, in the connections of well-insulated partitions without any obvious elements of high thermal transmittance, heat losses depend to a large extent on the shape of the junctions (Figure 8). The reduction in ψ values caused by the increase in insulating properties of the partitions is almost constant for all of the slopes and equal to 22%.

Table 6. Linear thermal transmittance (internal dimensions)—ridge.

Slope of the Roof [deg]	Linear Thermal Transmittance (Variant I) [W/(m·K)]	Linear Thermal Transmittance (Variant II) [W/(m·K)]
10	0.026	0.020
20	0.034	0.027
30	0.041	0.032
40	0.047	0.036

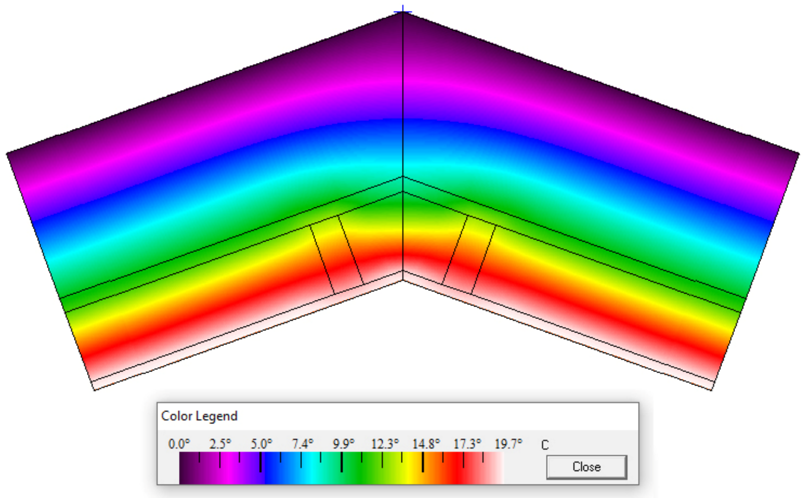

Figure 8. Schematic view of isotherms in the ridge junction (partitions cut closely to the center of the junction to make the figure smaller).

3.2. Heat Losses through an Exemplary Roof

The results of the analyses do not point unambiguously to what slope of a roof would be the most favorable regarding heat transfer. Smaller slopes show bigger heat flow through the knee wall–roof junction and smaller through the ridge, and in the case of bigger slopes, the situation is the opposite. The surface of the roof, differing for the examined slopes, may also have an important influence on the total heat transmission.

The following results (Tables 7–10) present heat loss coefficients H_{tr} for a gable roof 8 m wide and 12 m long (internal dimensions), shown in Figure 9.

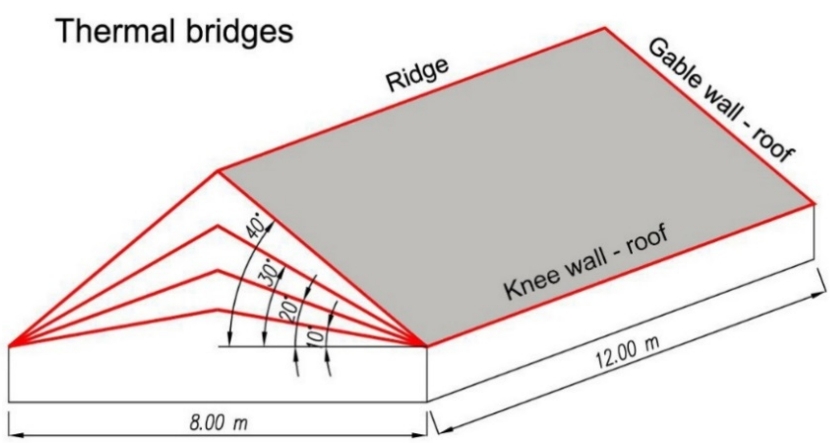

Figure 9. Outline of the roof and thermal bridges included in calculation of heat loss coefficients.

Table 7. Transmission heat loss coefficients for an exemplary gable roof, wall variant "I a".

Slope of the Roof [°]	Transmission Heat Loss Coefficient					
	Wall with Plaster to the Top			Wall with Plaster to the Level of the Ceiling		
	Total [W/K]	Thermal Bridges [W/K]	Thermal Bridges [%]	Total [W/K]	Thermal Bridges [W/K]	Thermal Bridges [%]
10	16.885	2.360	14.0	16.619	2.095	12.6
20	17.539	2.318	13.2	17.384	2.163	12.4
30	18.790	2.275	12.1	18.716	2.202	11.8
40	20.918	2.251	10.8	20.911	2.244	10.7

Table 8. Transmission heat loss coefficients for an exemplary gable roof, wall variant "I b".

Slope of the Roof [deg]	Transmission Heat Loss Coefficient					
	Wall with Plaster to the Top			Wall with Plaster to the Level of the Ceiling		
	Total [W/K]	Thermal Bridges [W/K]	Thermal Bridges [%]	Total [W/K]	Thermal Bridges [W/K]	Thermal Bridges [%]
10	17.019	2.494	14.7	16.739	2.214	13.2
20	17.675	2.454	13.9	17.557	2.336	13.3
30	18.974	2.460	13.0	18.915	2.401	12.7
40	21.111	2.444	11.6	21.103	2.436	11.5

Table 9. Transmission heat loss coefficients for an exemplary gable roof, wall variant "II a".

Slope of the Roof [°]	Transmission Heat Loss Coefficient					
	Wall with Plaster to the Top			Wall with Plaster to the Level of the Ceiling		
	Total [W/K]	Thermal Bridges [W/K]	Thermal Bridges [%]	Total [W/K]	Thermal Bridges [W/K]	Thermal Bridges [%]
10	13.399	1.994	14.9	13.134	1.729	13.2
20	13.906	1.954	14.0	13.758	1.806	13.1
30	14.878	1.910	12.8	14.812	1.844	12.4
40	16.559	1.901	11.5	16.551	1.893	11.4

Table 10. Transmission heat loss coefficients for an exemplary gable roof, wall variant "II b".

Slope of the Roof [deg]	Transmission Heat Loss Coefficient					
	Wall with Plaster to the Top			Wall with Plaster to the Level of the Ceiling		
	Total [W/K]	Thermal Bridges [W/K]	Thermal Bridges [%]	Total [W/K]	Thermal Bridges [W/K]	Thermal Bridges [%]
10	13.561	2.156	15.9	13.273	1.868	14.1
20	14.062	2.110	15.0	13.917	1.965	14.1
30	15.082	2.115	14.0	15.031	2.063	13.7
40	16.751	2.093	12.5	16.751	2.093	12.5

In the connection of the gable wall and roof, the ψ values were 0.045 W/(m·K) and 0.047 W/(m·K) (variant I), and 0.036 W/(m·K) and 0.039 W/(m·K) (variant II) for the wall construction types "a" and "b", respectively. The calculations include heat losses through the roof slope and thermal bridges along eaves, ridge, and the top of gable walls, according to Equation (3) [48]:

$$H_{tr} = \sum_i U_{ri} \cdot A_{ri} + \sum_j \psi_j \cdot L_j \tag{3}$$

where i—number of the roof slopes; U_r—thermal transmittance coefficient of the roof [W/(m^2·K)]; A—internal surface of a roof slope [m^2]; j—number of the thermal bridges; ψ—linear thermal transmittance of a thermal bridge [W/(m·K)]; L—internal length of a thermal bridge [m].

Transmission heat losses Q_{tr} [Wh] during a period depend proportionally on the heat loss coefficient, as in Equation (4) [48]:

$$Q_{tr} = H_{tr} \cdot (\theta_{int,H} - \theta_e) \cdot t_M \tag{4}$$

where $\theta_{int,H}$—the set-point temperature for heating [°C]; θ_e—mean external temperature during a period [°C]; t_M—duration of the calculation period [h].

The transmission heat loss coefficient clearly rises with the growing slope of the roof (Figure 10). The contribution of thermal bridges to the total heat loss coefficient ranges from 10.7% to 15.9%. It decreases as the slope of the roof increases, because of the rising impact of the heat losses through the growing roof area. For the wall variant "b", the influence is slightly higher, because of the higher values of the linear transmittance coefficients themselves. Using the construction with the load-bearing frame located at the internal wall surface enlarges heat losses from the roof by 1.1% on average. Improved insulation reduces the heat loss coefficient by 21% on average.

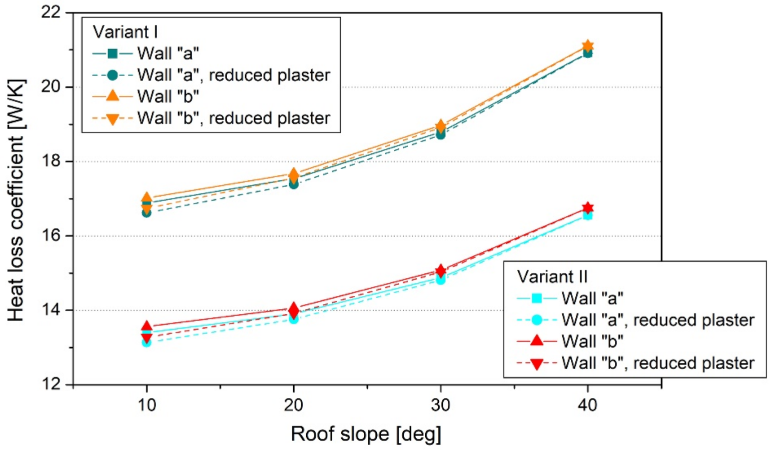

Figure 10. Heat loss coefficients of an exemplary roof.

Thanks to the modification of the bridges consisting of removing the plaster from their interior it is possible to lower the heat losses up to 1.6% in variant I and up to 2.1% in variant II (in the case of the slope of the roof 10°). This change has rather a limited effect on the heat transfer, lessening as the slope of the roof grows. However, it may be still worth taking into consideration as a solution not generating additional costs.

4. Conclusions

Hemp–lime composite is a material used to fill building partitions that have wooden load-bearing elements. It belongs to a group of ecological, recyclable, easy-to-prepare materials made of locally available components. Using this material in typical and low-energy buildings demands the assertion of the possibility of constructing building partitions and junctions characterized by low thermal transmittance. The presented research proves such potential of the composite—the U values of the walls and roof are in the range between 0.15 and 0.20 W/(m^2·K), and between 0.12 and 0.15 W/(m^2·K), respectively, and all of the analysed thermal bridges have ψ values well below 0.10 W/(m·K).

The study concentrates on thermal bridges appearing in roofs of different slopes and their connections with knee and gable walls. Our experiments enabled a comparison between different types of walls, concerning the heat transfer in construction junctions. The analyses revealed weak spots in the thermal bridges, which was a starting point for working out improved solutions with reduced linear thermal transmittance coefficients.

The final recommendations regarding the roof construction are as follows:

- The smaller tilt of a roof is a factor diminishing heat transfer through the main part of the construction;
- Even though they increase the heat transfer through the linear bridges, their influence is of minor importance in this case;
- As the share of the thermal bridges in the total heat losses may be up to 15%, the above statement does not justify the negligence of carefully designing the construction junctions, especially in low-energy buildings;
- Through the analyses of heat transfer in specific junctions, it is possible to identify weak points in construction and substitute them with an alternative, better design.

It is also worth mentioning that accounting for heat losses throughout the whole construction is an approach that gives more reliable and complete information compared with an examination of the thermal transmittance coefficients of isolated building partitions and junctions.

The presented work has some limitations. Firstly, the effects associated with the 3D heat flow in the rafters and roof insulation were neglected. In the presented case, the partitions are relatively uniform in terms of the thermal properties of its components, lowering the resulting simulation error. Also, the two-step modelling procedure was introduced, based on the substitution of non-uniform layers by the equivalent thermal conductivity, calculated with the use of additional 2D simulations. Secondly, in practical applications, the elements used in real constructions may have different thermal properties or dimensions, so the presented values of linear thermal transmittance coefficients or heat loss coefficients should be treated as approximates. Thirdly, vapor transfer is not included in the study, as it cannot be handled by computer programs meant for heat transfer analyses [49].

Author Contributions: Conceptualization, M.G. and P.B.; methodology, M.G. and P.B.; software, M.G.; validation, M.G.; formal analysis, M.G. and P.B.; investigation, M.G. and P.B.; resources, M.G. and P.B.; data curation, M.G. and P.B.; writing—original draft preparation, M.G., P.B., K.P. and W.J.; writing—review and editing, M.G., P.B., K.P. and W.J.; visualization, M.G., K.P. and W.J.; supervision, M.G. and P.B.; project administration, P.B.; funding acquisition, M.G., K.P., W.J. and P.B. All authors have read and agreed to the published version of the manuscript.

Funding: This research was funded by Polish Ministry of Education and Science within the grant numbers: FD-20/IL-4/022; FD-20/IL-4/009; FD-20/AU-1/029; FD-20/AU-1/022.

Data Availability Statement: Data is contained within the article.

Conflicts of Interest: The authors declare no conflicts of interest.

References

1. Alhavari, A.; Mukhopadhyaya, P. Thermal Bridges in Building Envelopes an Overview of Impacts and Solutions. *Int. Rev. Appl. Sci. Eng.* **2018**, *9*, 31–40. [CrossRef]
2. Building Performance Institute Europe (BPIE). *Renovation Strategies of Selected EU Countries: A Status Report on Compliance with Article 4 of the Energy Efficiency Directive*; BPIE: Brussels, Belgium, 2014. Available online: https://bpie.eu/wp-content/uploads/2015/10/Renovation-Strategies-EU-BPIE-2014.pdf (accessed on 21 November 2023).
3. Yuan, X.; Wang, X.; Zuo, J. Renewable energy in buildings in China—A review. *Renew. Sustain. Energy Rev.* **2013**, *24*, 1–8. [CrossRef]
4. Brzyski, P.; Grudzińska, M.; Majerek, D. Analysis of the Occurrence of Thermal Bridges in Several Variants of Connections of the Wall and the Ground Floor in Construction Technology with the Use of a Hemp–Lime Composite. *Materials* **2019**, *12*, 2392. [CrossRef]

5. Pérez-Lombard, L.; Ortiz, J.; Pout, C. A review on buildings energy consumption information. *Energy Build.* **2008**, *40*, 394–398. [CrossRef]
6. The United Nations. Paris Agreement. 2015. Available online: https://unfccc.int/sites/default/files/english_paris_agreement.pdf (accessed on 21 November 2023).
7. European Parliament. Directive 2002/91/EC of the European Parliament and of the Council of 16 December 2002 on the Energy Performance of Buildings. *Off. J. Eur. Union* **2003**, *46*, 65–71. Available online: https://eur-lex.europa.eu/LexUriServ/LexUriServ.do?uri=OJ:L:2003:001:0065:0071:en:PDF (accessed on 21 November 2023).
8. European Parliament. Directive 2023/955/EU of the European Parliament and the Council of 30 May 2018 on the Energy Perfromance of Buildings. *Off. J. Eur. Union* **2023**. Available online: https://eur-lex.europa.eu/legal-content/EN/TXT/HTML/?uri=CELEX:32023L1791&qid=1700576301961 (accessed on 21 November 2023).
9. Trotta, G. Assessing energy efficiency improvements, energy dependence, and CO_2 emissions in the European Union using a decomposition method. *Energy Effic.* **2019**, *12*, 1873–1890. [CrossRef]
10. Theodosiou, T.G.; Papadopoulos, A.M. The impact of thermal bridges on the energy demand of buildings with double brick wall constructions. *Energy Build.* **2008**, *40*, 2083–2089. [CrossRef]
11. Kotti, S.; Teli, D.; James, P.A.B. Quantifying Thermal Bridge Effects and Assessing Retrofit Solutions in a Greek Residential Building. *Procedia Environ. Sci.* **2017**, *38*, 306–313. [CrossRef]
12. Evola, G.; Margani, G.; Marletta, L. Energy and cost evaluation of thermal bridge correction in Mediterranean climate. *Energy Build.* **2011**, *43*, 2385–2393. [CrossRef]
13. Ilomets, S.; Kalamees, T. Evaluation of the criticality of thermal bridges. *J. Build. Pathol. Rehabil.* **2016**, *1*, 11. [CrossRef]
14. Dumitrescu, L.; Baran, I.; Pescaru, R.A. The Influence of Thermal Bridges in the Process of Buildings Thermal Rehabilitation. *Procedia Eng.* **2017**, *181*, 682–689. [CrossRef]
15. Brzyski, P.; Grudzińska, M.; Böhm, M.; Łagód, G. Energy Simulations of a Building Insulated with a Hemp-Lime Composite with Different Wall and Node Variants. *Energies* **2022**, *15*, 7678. [CrossRef]
16. Jedidi, M.; Benjeddou, O. Effect of Thermal Bridges on the Heat Balance of Buildings. *Int. J. Civ. Eng.* **2018**, *2*, 41–49.
17. Mayer, Z.; Kahn, J.; Götz, M.; Hou, Y.; Beiersdörfer, T.; Blumenröhr, N.; Volk, R.; Streit, A.; Schultmann, F. Thermal Bridges on Building Rooftops. *Sci. Data* **2023**, *10*, 268. [CrossRef]
18. Cox-Ganser, J.M. Indoor dampness and mould health effects—Ongoing questions on microbial exposures and allergic versus nonallergic mechanisms. *Clin. Exp. Allergy* **2015**, *45*, 1478–1482. [CrossRef]
19. Grudzińska, M.; Brzyski, P. The Occurrence of Thermal Bridges in Hemp-Lime Construction Junctions. *Period. Polytech. Civ. Eng.* **2019**, *63*, 377–387. [CrossRef]
20. Borgero, S.; Chiari, A. The influence of thermal bridge calculation method on the building energy need: A case study. *Energy Procedia* **2018**, *148*, 1042–1049. [CrossRef]
21. Kosiński, P.; Brzyski, P.; Tunkiewicz, M.; Suchorab, Z.; Wiśniewski, D.; Palczyński, P. Thermal Properties of Hemp Shives Used as Insulation Material in Construction Industry. *Energies* **2022**, *15*, 2461. [CrossRef]
22. Meshgin, P.; Xi, Y. Multi-scale composite models for the effective thermal conductivity of PCM-concrete. *Constr. Build. Mater.* **2013**, *48*, 371–378. [CrossRef]
23. Li, H.; Zeng, Q.; Xu, S. Effect of pore shape on the thermal conductivity of partially saturated cement-based porous composites. *Cem. Concr. Compos.* **2017**, *81*, 87–96. [CrossRef]
24. Qiu, L.; Zou, H.; Tang, D.; Wen, D.; Feng, Y.; Zhang, X. Inhomogeneity in pore size appreciably lowering thermal conductivity for porous thermal insulators. *Appl. Therm. Eng.* **2018**, *130*, 1004–1011. [CrossRef]
25. Li, K.; Li, D.; Liu, D. Meso-scale investigations on the effective thermal conductivity of multi-phase materials using the finite element method. *Int. J. Heat Mass Transf.* **2020**, *151*, 119383. [CrossRef]
26. Sinka, S.; Sahmenko, G.; Korjakins, A.; Radina, L.; Bajare, D. Hemp Thermal Insulation Concrete with Alternative Binders, Analysis of their Thermal and Mechanical Properties. *IOP Conf. Ser. Mater. Sci. Eng.* **2015**, *96*, 012029. [CrossRef]
27. Pietruszka, B.; Gołębiewski, M. Właściwości wyrobów budowlanych na bazie konopi. *Przegląd Bud.* **2019**, *10*, 139–141.
28. Walker, R.; Pavía, S. Moisture transfer and thermal properties of hemp–lime concretes. *Constr. Build. Mater.* **2014**, *64*, 270–276. [CrossRef]
29. Elfordy, S.; Lucas, F.; Tancret, F.; Scudeller, Y.; Goudet, L. Mechanical and thermal properties of lime and hemp concrete ("hempcrete") manufactured by a projection process. *Constr. Build. Mater.* **2008**, *22*, 2116–2123. [CrossRef]
30. Barnat-Hunek, D.; Smarzewski, P.; Fic, S. Mechanical and thermal properties of hemp-lime composites. *Compos. Theory Pract.* **2015**, *15*, 21–27.
31. Evrard, A. Sorption behaviour of Lime-Hemp Concrete and its relation to indoor comfort and energy demand. In Proceedings of the PLEA2006—23rd International Conference on Passive and Low Energy Architecture, Geneva, Switzerland, 6–8 September 2006.
32. Bevan, R.; Wolley, T. Hemp lime construction. In *A Guide to Building with Hemp Lime Composites*; IHS BRE Press: Bracknell, UK, 2008; ISBN 978-1-84806-033-3.
33. Bevan, R.; Wolley, T. Constructing aa low energy house from hempcrete and other natural materials. In Proceedings of the 11th International Conference on Non-conventional Materials and Technologies (NOCMAT 2009), Bath, UK, 6–9 September 2009.

34. Florentin, Y.; Pearlmutter, D.; Givoni, B.; Gal, E. A life-cycle energy and carbon analysis of hemp-lime bio-composite building materials. *Energy Build.* **2017**, *156*, 293–305. [CrossRef]
35. Schiavoni, S.; D'Alessandro, F.; Bianchi, F.; Asdrubali, F. Insulation materials for the building sector: A review and comparative analysis. *Renew. Sustain. Energy Rev.* **2016**, *62*, 988–1011. [CrossRef]
36. *ISO 10211*; Thermal Bridges in Building Construction. Heat Flows and Surface Temperatures. Detailed Calculations. European Committee for Standardization: Geneva, Switzerland, 2017.
37. Available online: https://windows.lbl.gov/software-tools (accessed on 13 November 2023).
38. Hilderson, W. Therm 7.4 Validation According to EN ISO 10211:2007. The Flemish Passive House Platform. Available online: https://pixii.be/sites/default/files/therm_7.4_validatie_10211.pdf (accessed on 13 November 2023).
39. Garay, R.; Uriarte, A.; Apraiz, I. Performance assessment of thermal bridge elements into a full scale experimental study of a building façade. *Energy Build.* **2014**, *85*, 579–591. [CrossRef]
40. Kempton, L.; Kokogiannakis, G.; Green, A.; Cooper, P. Evaluation of thermal bridging mitigation techniques and impact of calculation methods for lightweight steel frame external wall systems. *J. Build. Eng.* **2021**, *43*, 102893. [CrossRef]
41. Ramalho de Freitas, J.; Grala da Cunha, E. Thermal bridges modeling in South Brazil climate: Three different approaches. *Energy Build.* **2018**, *169*, 271–282. [CrossRef]
42. Smusz, R.; Korzeniowski, M. Experimental investigation of thermal bridges in building at real conditions. *E3S Web Conf.* **2018**, *70*, 03013. [CrossRef]
43. *ISO 6946*; Building Components and Building Elements. Thermal Resistance and Thermal Transmittance. Calculation Methods. European Committee for Standardization: Geneva, Switzerland, 2017.
44. Nagy, B. Comparative analysis of multi-dimensional heat flow modeling. In Proceedings of the 2nd Conference for PhD Students in Civil Engineering, Cluj-Napoca, Romania, 10–12 December 2014.
45. *ISO 10456*; Building Materials and Products—Hygrothermal Properties—Tabulated Design Values and Procedures for Determining Declared and Design Thermal Values. European Committee for Standardization: Geneva, Switzerland, 2007.
46. Available online: https://imgw.pl/wydarzenia/warunki-termiczne-w-polsce-w-sezonie-zimowym-20202021 (accessed on 22 December 2023).
47. *ISO 14683*; Thermal Bridges in Building Construction. Linear Thermal Transmittance. Simplified Methods and Default Values. European Committee for Standardization: Geneva, Switzerland, 2017.
48. *ISO 52016-1*; Energy Performance of Buildings. Energy Needs for Heating and Cooling, Internal Temperatures and Sensible and Latent Heat Loads. Part 1: Calculation Procedures. European Committee for Standardization: Geneva, Switzerland, 2017.
49. Nagy, B.; Marosvölgyi, M.; Szalay, M. Comparison of thermal bridge calculation methods. *Acta Polytech. CTU Proc.* **2022**, *38*, 77–83. [CrossRef]